Proceedings of the 2023 International Conference on Machine Learning and Automation
DOI: 10.54254/2755-2721/41/20230702

Control strategies modeling for robotic exoskeletons facilitating Sit-to-Stand transitions in geriatric and lower limb impaired

Kailun Zhang

Polytechnic Institute, 110 8th St, Troy, NY, 12180, United States

zhangk9@rpi.edu

Abstract. With the growing global aging population, there's been an amplified societal emphasis on preserving the health of the elderly and enhancing their quality of life. In this scenario, robotic exoskeletons have emerged as a cutting-edge solution to assist the elderly and those with lower limb muscle deficiencies in Sit-to-Stand (STS) exercises. These exoskeletons adopt two main approaches: full assistance for those with entirely weakened lower limbs and partial assistance for those with some remaining muscle strength. This article introduces two modeling methods and concepts for these control strategies, aligning with the full and partial assistance directions, respectively. Both approaches hinge on the Lagrange equation as their foundational structure, integrating distinct kinematic designs to form their individual dynamic models. Based on this, the models are further adapted to address the specific risks associated with STS activities as per each strategy. Research outcomes highlight that by assessing the wearer's EMG signal, the partial assistance strategy considerably mitigates the lower limb muscle strength required for STS under conditions such as low-speed, medium-speed, sitback-like, and step-like. This not only improves balance but also augments the likelihood of successful STS execution, consequently diminishing fall incidents.

Keywords: Robots Exoskeleton, Sit-to-Stand, Modeling.

1. Introduction

With the progression of technology and improvements in the quality of life, global populations are experiencing extended lifespans. This has led to a noticeable increase in the elderly population across all nations, indicating an upward trajectory. Given the aim of aiding senior individuals in upholding a healthy lifestyle and mitigating the adverse effects of prolonged muscular inactivity, basic activities like walking become indispensably essential. Nevertheless, the act of transitioning from a seated to a standing position, which involves rising from a chair without losing balance, proves to be more demanding than activities like walking, even a slight lapse in attention can lead to falls and subsequent injuries, particularly as the body ages [1], [2]. Hence, taking into account the risks posed by falls to the elderly and stroke patients, robotic exoskeletons have emerged as a widely embraced remedy.

Due to the potential risks of unstable sitting and standing motions leading to injuries like falls, it is of paramount importance to investigate exoskeleton control strategies capable of delivering dependable assistance for STS transitions. Considering the patient's specific condition, STS assistance strategies can be broadly categorized. For patients belonging to the first group, characterized by minimal or negligible

© 2023 The Authors. This is an open access article distributed under the terms of the Creative Commons Attribution License 4.0 (https://creativecommons.org/licenses/by/4.0/).

DOI: 10.54254/2755-2721/41/20230702

lower limb muscle strength, the exoskeleton assumes the responsibility for generating all the necessary torque. This subgroup is entirely reliant on exoskeletons for their mobility, whereby users issue commands while the exoskeleton assumes the role of execution leader. A prevalent approach involves manually creating trajectories using previously captured human motion data [3], [4], incorporating joint position and joint velocity information, and then simplifying and generating summarized models. Simultaneously, it is crucial to uphold equilibrium for this specific group of patients, often necessitating the evaluation of the wearer's Center of Mass (CoM) to gauge their STS stability and guide the creation of reference trajectories. However, it's worth noting that this method primarily applies to scenarios where significant kinematic and mass attribute disparities between exoskeletons and humans are absent. Its primary objective is to assist wearers in successfully executing STS movements without factoring in their voluntary capabilities. As a result, this approach might not fully harness the complete range of abilities and advantages offered by exoskeletons.

Within the second user category encompassing individuals with partial muscle strength, like the elderly and stroke patients, the exoskeleton primarily facilitates STS movements by augmenting joint strength. For this subgroup, capable of specific activities, enhanced flexibility, reduced injury risk, and potential rehabilitation support are essential. In this context, user agency takes precedence, with the exoskeleton and control system harmonizing the wearer's muscle actions. From a rehabilitation and flexibility perspective, the crux of the STS assistance strategy lies in real-time movement intention estimation, giving rise to various methods in existing literature. One such approach involves segmenting the STS motion into distinct sub-stages and using threshold-based [5] or machine learning-driven calculations to detect transitions [6]. To ensure the ongoing estimation of movement intent, the joint torque generated by the wearer frequently serves as a representative indicator, commonly assessed through techniques such as electromyography (EMG) and force/torque sensors [7]. Despite their high accuracy, these methods bear two drawbacks: EMG sensors' sensitivity to multiple factors leading to intricate calibration, and the elevated cost associated with compact design torque/force sensors.

This paper aims to introduce and analyze an existing control strategy selected from the two distinct types of STS assistance strategies. The first control strategy provides comprehensive assistance to users of the Atalante exoskeleton. It employs constrained trajectory optimization and nonlinear control to realize trajectories based on a high degree of freedom (DOF) model. This strategy introduces a novel approach to selecting control objectives for highly constrained systems, ensuring compatibility with contact constraints. Additionally, it successfully passes robustness tests involving various scenarios, such as different users, chair heights, zero user force, spasticity in the knee joints, and asymmetric motor torque output [8]. The second control strategy focuses on assisting STS motions for individuals with partial motor ability. It incorporates an impedance model and an impedance modulation structure, enabling balance-enhanced control. This approach ensures appropriate strength and balance assistance according to the wearer's STS posture and speed, effectively reducing human effort. Moreover, it addresses the avoidance of two common failed STS movements, namely sitbacks and steps, caused by insufficient balance and coordination [9].

2. Method

This article will present the initial control assistance strategy utilizing the work of Mungai et al., followed by an introduction to the subsequent control assistance strategy based on the research by Huo et al.

2.1. The First control assistance strategy

Developing an effective control system often necessitates the formulation of control objectives to facilitate subsequent design, computation, and simulation. The initial type of control strategy commonly focuses on individuals with lower limb paralysis, rendering them incapable of providing lower body strength. While some paralyzed patients might have the capacity to employ their hands, crutches, or rely on external assistance for support, this strategy opts for simplification in modeling and control system design. It also seeks to cater to a broader user spectrum. Under this approach, it is assumed that the

DOI: 10.54254/2755-2721/41/20230702

application of force by users to the chair's armrests does not generate any torque (within the body's reference frame). Furthermore, for the sake of streamlining the model for power generation systems, a rigid connection and transmission system are presumed. In this scenario, the exoskeleton must fully control the STS process, imitating and performing the role of lower limbs during a typical STS exercise. Consequently, this initial control strategy revolves around completely assisted exoskeletons, exemplified by hardware like the Atalante.

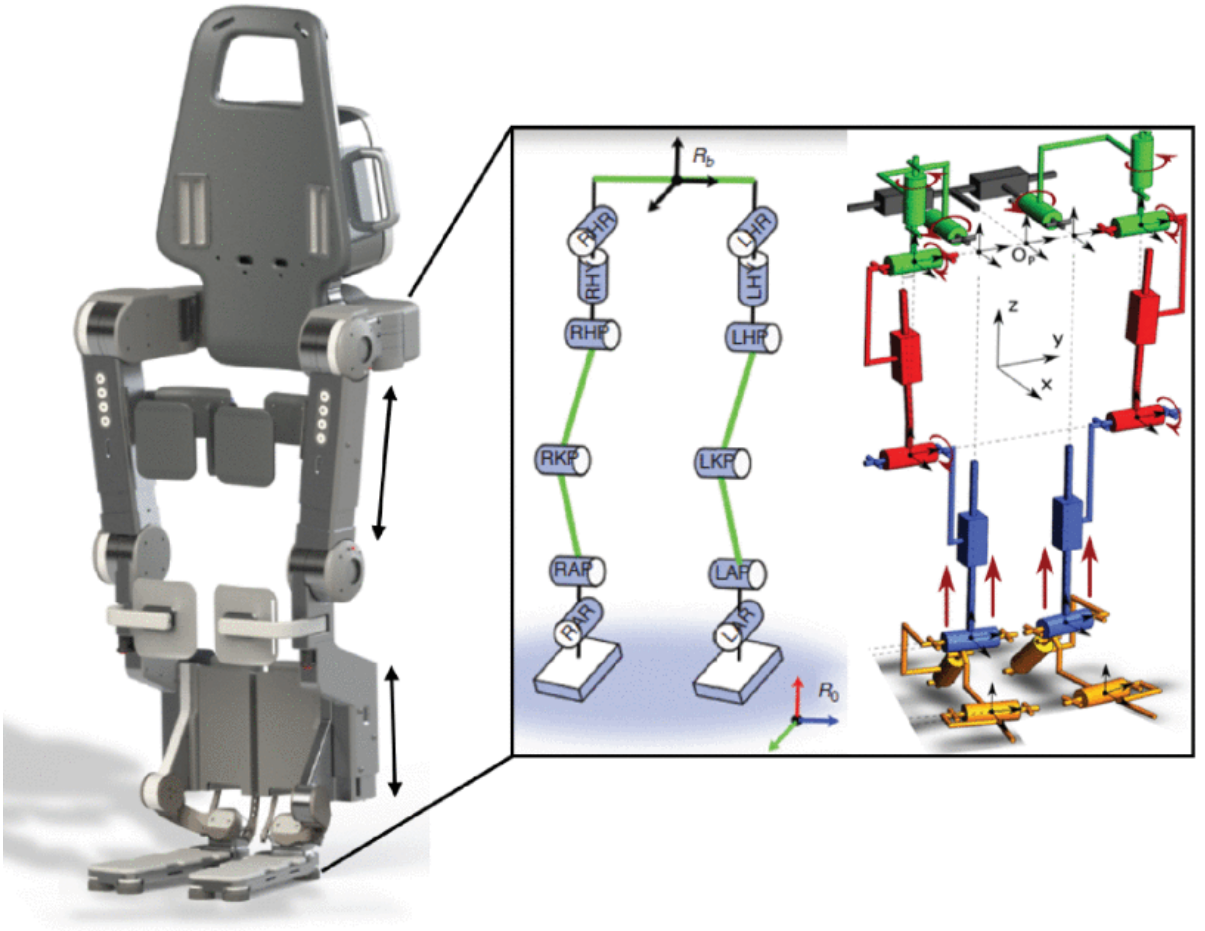

Figure 1. Kinematics architecture of Atalante [10].

The exoskeleton incorporates one driving joint at each of the six joints within each leg, resulting in a total of 12 DOF. When considering the standard six DOF encompassing position and rotation in three-dimensional space, this exoskeleton boasts a combined 18 DOF. While a higher DOF enhances the potential range of motion, it concurrently amplifies the intricacies involved in modeling and control systems. Consequently, the generalized coordinate vector required by the model assumes the form of an 18x1 matrix, representing each mobile joint. During exoskeleton operation, the control system must comprehend various physical attributes, including the torque input vector, inertia, Coriolis effects, force matrices/vectors, friction arising from contact between the exoskeleton, floor, and seat, and the force contributed by the user. Ultimately, taking into account the fact that the robot's exoskeleton is categorized as a floating base, and in conjunction with the application of the Lagrange method within the domain of mechanical dynamics, a dynamic model was formulated. This model aptly encapsulates the motor's inertia and transmission mechanism with respect to the associated links [11].

$$D(q)\ddot{q} + C(q,\dot{q})\dot{q} + G(q) = Bu + J^T(q)\Gamma + J_{ext}^T\zeta \tag{1}$$

DOI: 10.54254/2755-2721/41/20230702

$$J(q)\ddot{q} + \dot{J}(q,\dot{q})\dot{q} = 0 \tag{2}$$

where q is the vector of generalized coordinates, u is the torque input vector, D, C, and G are the inertia, Coriolis, and gravity matrices/vector, respectively, B is the torque distribution matrix, J is the Jacobian mapping the contact wrenches to the generalized coordinates, Γ is the contact wrench associated with the exoskeleton's contact with the floor and the seat of the chair, ζ is the force provided by the user, and J_{est} is the jacobian that maps the provided user force to the generalized coordinates. Equation (2) gives the lagrange multipliers (Γ) that are necessary to enforce the contact constraints.

Furthermore, the initial form of control strategy divides the motion within the STS process into a hybrid model that encompasses both the seated and standing domains. This model introduces a total of three points of contact within the seated region: the chair, the right foot, and the left foot. Meanwhile, the standing region involves two contact points solely for the feet, one on the right and the other on the left. The shift from the seated to the standing area is determined by the absence of any interaction between the mechanical exoskeleton and the chair. This transition is mathematically indicated when the vertical force component exerted by the seat reaches 0, thereby prompting the system to initiate the switch between these two distinct domains.

Throughout the STS process, the maintenance of user stability is paramount, necessitating the careful management of the Zero Moment Point (ZMP) [12], [13]. This ZMP reference point must be maintained within a suitable range to avert the risk of user falls. When the user is actively engaging force or in contact with the chair, this range encompasses both the chair's feet and those of the exoskeleton. Conversely, when the user is not applying force or in contact with the chair, the range is confined to the exoskeleton's feet alone. The computation of the ZMP involves the establishment of a spatial framework. Within this spatial context, the precise ZMP location is determined by the calculation of the point on the ground where the cumulative moments along the x and y axes equate to zero. The total moment $\tau = [\tau^x, \tau^y, \tau^z]^{\mathrm{T}}$ is given by

$$\tau := \sum_{i=1}^{N} (P_i - P_*) \times F_i^z + M_{total} \tag{3}$$

where N is the number of active contact points, $M_{total} = [M_{total}^x, M_{total}^y, M_{total}^z]^{\mathrm{T}}$ is the sum of all external moments, $P_i = [P_i^x, P_i^y, P_i^z]^{\mathrm{T}}$ is the point of application of the i -th contact force F_i, $P_* = [P_*^x, P_*^y, P_*^z]^{\mathrm{T}}$ is the unique point on the ground resulting in $\tau = [0,0,\tau^z]^{\mathrm{T}}$. That is, at P_* the moment is acting about an axis normal to the ground plane.

2.2. The second control assistance strategy

In contrast to the initial control approach, the second strategy is primarily oriented towards aiding individuals with lower limb mobility challenges who require support during STS motions. Analogous to the first control strategy, the second variant simplifies matters by presuming a rigid linkage between the exoskeleton and the user. It focuses solely on the subject's STS movement while excluding external force assistance.

In a general context, the lower extremities consist of three primary segments: the hip, knee, and ankle. These three segments are responsible for generating the highest levels of torque during STS motions. To streamline design and facilitate user muscle engagement, the second variant of the control strategy predominantly manages the torques generated by motors at the hip, knee, and ankle. This serves to mitigate the wearer's effort across these three regions during STS activities. As a result, the second control strategy employs a three DOF model for the human exoskeleton, wherein the lower limb exoskeleton—comprising the lower leg, thigh, and torso—is conceptualized as a triple inverted pendulum [14], [15].

DOI: 10.54254/2755-2721/41/20230702

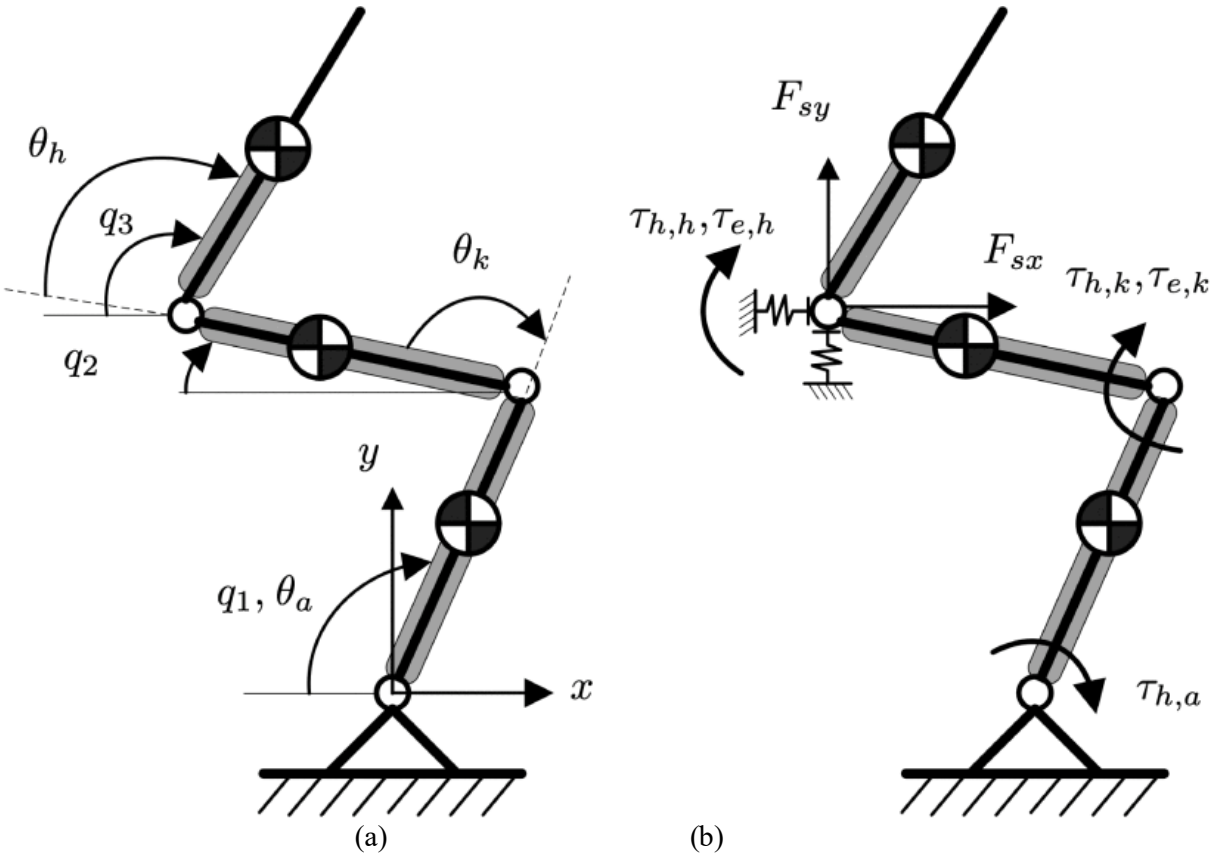

Figure 2. A diagram depicting a subject wearing an exoskeleton and successfully performing an STS movement in the sagittal plane. The exoskeleton is depicted as gray rounded rectangles.

Due to its three DOF, the matrix featuring a 1x3 angle state vector corresponds sequentially to the ankle joint, knee joint, and hip joint. Analogous to the initial control strategy, this model incorporates the input torque vector, inertia matrix, Coriolis and centripetal matrix, and gravitational vector into the dynamic framework. The distinction lies in the wearer of the second control strategy contributing torque, necessitating the harmonization of various vectors within the dynamic model with those generated by the user's provided torque. Additionally, this approach introduces the concept of seating force. In the second control strategy, the primary purpose of the seating force is to offset the gravitational load when the wearer is seated. This design counteracts the horizontal torque induced by gravity on the knee and ankle joints while the user is seated, thereby allowing free movement of the knee and ankle joints. Nevertheless, the seating force gradually decreases to zero during STS exercises.

The challenge here revolves around accurately interpreting the wearer's intention. Initially, the method considered setting the hip joint position as the detachment point and monitoring the detachment point's height to decide whether to reduce the seating force. Nevertheless, practical discrepancies in seat height can impede the system's ability to ascertain the unseating point position via joint angle data. Consequently, the method introduces the concept of synchronizing the maximum vertical ground reaction force (GRF) time with the "unseating" time and devises a seating force model. This model regulates the necessary output seating force by leveraging the ratio of the current vertical GRF (measured in real time) to the maximum vertical GRF. A smaller ratio results in a diminished output seating force, while a larger ratio leads to an amplified output seating force.

Integrate the seating force model into the preceding triple inverted pendulum framework, culminating in the derivation of the ultimate dynamic model for the robot exoskeleton employing the Euler-Lagrange formalism [16].

DOI: 10.54254/2755-2721/41/20230702

$$M(q)\ddot{q} + C(q,\dot{q})\dot{q} + G(q) = U + J_F^T F \tag{4}$$

where $q = [q_1\ q_2\ q_3]^T$ represents the state vector of the ankle, knee, and hip joint angles. $M(q)$, $C(q,\dot{q})$, and $G(q)$ denote the inertia matrix, the Coriolis and centrifugal matrix, and the gravitational vector, respectively. The seat force is modeled as an external force, F, that acts on the hip joint of the human–exoskeleton. J_F is the Jacobian matrix. The input torque vector U is given as follows:

$$U = U_h + U_e = R\left(\begin{bmatrix}\tau_{h,a}\\ \tau_{h,k}\\ \tau_{h,h}\end{bmatrix} + \begin{bmatrix}0\\ \tau_{e,k}\\ \tau_{e,h}\end{bmatrix}\right) \tag{5}$$

U_h denotes the vector of torques generated by the wearer at the ankle, knee, and hip joints. U_e represents the vector of torques exerted by the exoskeleton at the knee and hip joint levels. Note that both ankle joints of the exoskeleton are passive. The transformation matrix R is given as follows:

$$R = (J_\Theta^{-1})^T \tag{6}$$

where J_Θ represents the transformation matrix from the joint space $(\theta_a, \theta_k, \theta_h)$ to the defined joint angle space (q_1, q_2, q_3). The design of the seat force model is as follows:

$$F = [F_{sx}\ F_{sy}]^T = \beta_F F_s \tag{7}$$

With

$$\beta_F = 1 - F_{GRF}/F_{GRF,max}$$

where β_F is a positive ratio ($\beta_F \in [0\ 1]$). F_{GRF} denotes the measured vertical GRF, while $F_{GRF,max}$ represents the maximum vertical GRF. F_s is the force that can fully compensate for the torques at the wearer's ankle and knee joint levels induced by the body gravity and is calculated as follows:

$$F_s = (HR^{-1}J_F^T)^{-1}HR^{-1}G(q) \tag{8}$$

where H is a constant matrix used to extract the ankle and knee joint torques from the torque vector U.

In the alternate control strategy, building upon the foundational model discussed earlier, this approach introduces an impedance model aimed at mitigating the challenges associated with diminished lower limb muscle strength and compromised balance control often observed in the STS motion of elderly individuals and patients with neurological conditions.

When engaging in STS exercises, generating sufficient joint torque within the lower limbs poses a significant hurdle, particularly for individuals with weakened leg muscles. An effective remedy to this issue involves a partial counterbalance of the gravitational and inertial forces, achieved through impedance modulation within the human exoskeleton system. This approach holds the advantage of aiding the wearer in executing STS motions via compensatory mechanisms. This assistance enables the wearer to retain a dominant role during the STS process while concurrently facilitating the rehabilitation and strengthening of their lower limb muscles.

Drawing upon the human exoskeleton model (4), a compensation model rooted in impedance is proposed, tailored to the wearer's specific lower limb mobility capabilities. This model is formulated as follows:

$$\lambda_1(\mathrm{M(q)}\ddot{q}_r + \mathrm{C(q,\dot{q})}\dot{q}_r) + \lambda_2\mathrm{G(q)} = \mathrm{R}\hat{\tau}_h + \lambda_2 J_F^T F \tag{9}$$

with

$$\lambda_1 = \lambda_2 = \mathrm{diag}(1, \lambda_k, \lambda_h), \quad \lambda_k, \lambda_h \in (0,1] \tag{10}$$

where the vectors $\ddot{q}_r$ and $\dot{q}_r$ denote the generated reference joint accelerations and velocities, respectively. $\hat{\tau}_h$ represents the estimated wearer's joint torques vector. λ_k and λ_h represent the assistive ratios at the hip and knee joint levels, respectively.

DOI: 10.54254/2755-2721/41/20230702

To address the challenge of insufficient wearer balance control, this approach employs coordinated adjustments in the movements of lower limb joints. A solution is introduced wherein virtual stiffness is implemented at the user's Head, Arms, and Trunk (HAT) level to mitigate balance loss. This is achieved by establishing a segmented function denoted as F_v, contingent upon the CoM position in the horizontal plane. This function governs the magnitude of the resultant virtual stiffness, denoted as F_v. Within this function, X_{CoM} is confined within a specified range relative to the foot position (origin). When X_{CoM} falls within this range, the system interprets no requirement for virtual stiffness (F_v = 0), granting the wearer freedom to adjust their posture unrestrictedly. However, once the X_{CoM} surpasses this designated range, the system activates virtual stiffness proportionate to the extent of the deviation from the prescribed range. This corrective measure assists the wearer in returning to the predetermined range, effectively averting balance loss and potential falls. The formulated segmented function is outlined as follows:

$$F_v = \begin{cases} -\mathrm{F}_{1max}\tanh\left(\mathrm{K}_{s1}(X_{CoM} - x_{c1})\right), & \text{if } X_{CoM} < x_{c1} \\ 0, & \text{if } x_{c1} \leq X_{CoM} \leq x_{c2} \\ -\mathrm{F}_{2max}\tanh\left(\mathrm{K}_{s2}(X_{CoM} - x_{c2})\right), & \text{if } X_{CoM} > x_{c2} \end{cases} \tag{13}$$

where F_{1max} and F_{2max} represent the maximum virtual stiffness forces, and K_{s1} and K_{s2} are the sensitive gains. X_{CoM} denotes the horizontal position of the CoM of the human–exoskeleton system in the sagittal plane. x_{c1} and x_{c2}, respectively, represent the virtual left and right margins of X_{CoM}, with $x_{c1} \leq 0 \leq x_{c2}$.

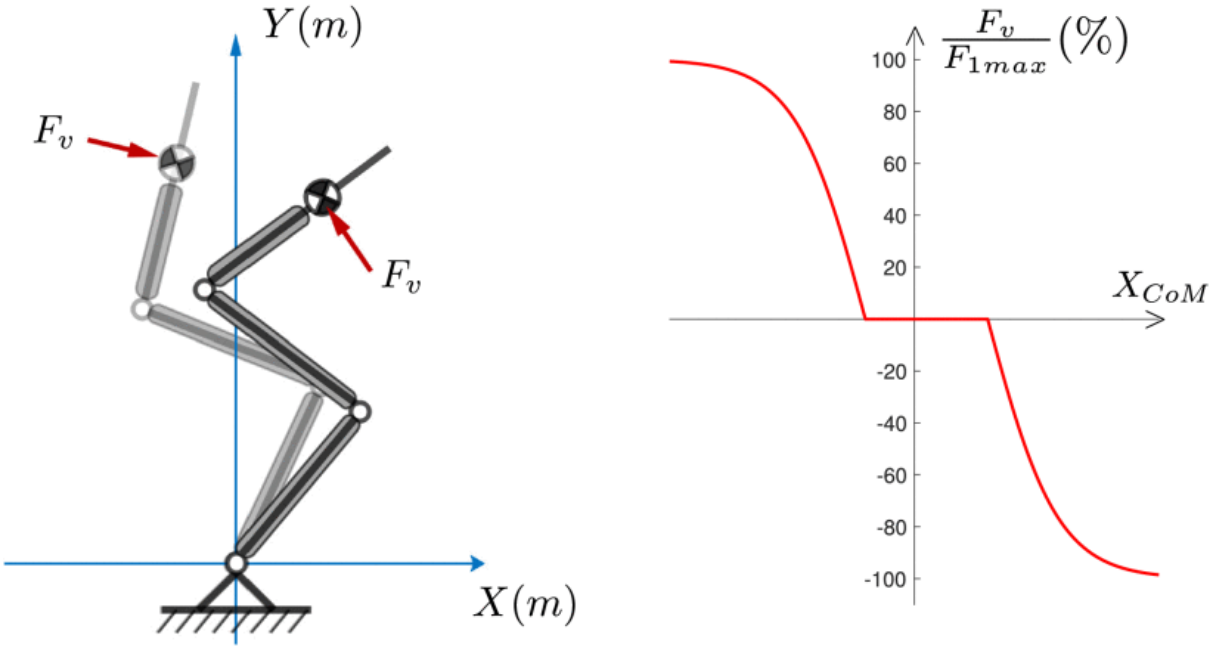

(a) (b)

Figure 3. Principle diagram of the virtual stiffness force (VSF). (a) VSF directions. (b) Example curve of the VSF (with $F_{1max} = F_{2max}$ and $K_{s1} = K_{s2}$).

By combining the virtual stiffness force and the impedance compensation (i.e., (9)), the desired impedance model can be expressed as follows:

$$\lambda_1(\mathrm{M}(\mathrm{q})\ddot{q}_r + \mathrm{C}(\mathrm{q},\dot{\mathrm{q}})\dot{q}_r) + \lambda_2\mathrm{G}(\mathrm{q}) = \mathrm{R}(\hat{\tau}_h + \tau_v) + \lambda_2 J_F^T F \tag{12}$$

with

DOI: 10.54254/2755-2721/41/20230702

$$\tau_v = \frac{F_{GRF}(1-\lambda_h)}{F_{GRF,max}(1-\delta_k-\lambda_{k0})}[0 \quad 0 \quad F_v l_3 k_{h3}]^T \tag{13}$$

where τ_v represents the virtual torque caused by the virtual stiffness force (11); $\| \tau v \| < \varepsilon_v$. ε_v is a positive constant. The virtual torque τ_v is also defined as a function of the GRF F_{GRF} and the assistive ratio λ_h. δ_k and λ_{k0} are two constants determining the middle and range of ratios λ_h and λ_k, respectively. Note that the virtual torque is considered to be zero when the wearer sits on a chair, i.e., F_{GRF}=0, or when the assistive ratio λ_h=1.

2.3. Conclusion

When comparing the two categories of control strategies, despite the first category concentrating on fully assisted wearers and the second on semi-assisted wearers, both strategies employ Lagrange equations instead of Newton's laws of motion in dynamic modeling. This choice is underpinned by the inherent advantages of the Lagrange equation: it furnishes a comprehensive framework applicable to various physical systems without necessitating adjustments to formalism for specific cases. Within the Lagrangian, the system's dynamics are encapsulated, and the equation of motion naturally emerges from action's minimization or maximization. The Euler-Lagrange equation seamlessly accommodates generalized coordinates, which are notably more adaptable than Cartesian coordinates for intricate systems. This renders it particularly suitable for challenges involving constraints and systems characterized by a significant number of DOF.

Furthermore, both the first and second approaches incorporate the concept of gauging vertical forces exerted either by the chair or the ground to ascertain the wearer's STS progression. Nonetheless, when contrasted with the first method that directly establishes the conversion criterion as a vertical component of 0, the second method employs a ratio-based technique to progressively adjust the generated seating force. This method facilitates a more gradual integration of the mechanical exoskeleton's assistance throughout the STS movement, enhancing the wearer's acclimation and reducing the likelihood of falls, all while improving overall comfort.

In the context of fall prevention, the initial control strategy safeguards user equilibrium and averts potential falls by managing the overall ZMP within a confined scope. This approach offers the benefit of granting the exoskeleton greater maneuverability to sustain balance, thus enhancing its fault tolerance. Conversely, the second control strategy establishes an initial range and subsequently monitors the CoM position within the human exoskeleton system to determine the necessity of applying virtual stiffness to avert falls. The advantage here is that within the designated range, the exoskeleton refrains from imposing any virtual stiffness, empowering users with greater freedom to execute diverse movements. When the CoM shifts beyond the designated range, the system can promptly introduce suitable virtual stiffness commensurate with the deviation magnitude, assisting the CoM's return to a secure range and thwarting potential falls.

3. Results

In this chapter, this article will primarily focus on introducing and analyzing the experimental outcomes associated with the second control strategy.

The second control strategy primarily aimed to assess the effectiveness of two common STS strategies: low speed (completed within 15 seconds) and medium speed (completed within 8 seconds), as well as two typical modes of STS failure in elderly individuals, attributed to a lack of muscle strength and balance control ability, namely, the sitback and step modes.

This approach involved using EMG signals measured by testing and comparing the VL and BF muscles in the experimenter's legs, as well as the ES muscles, to evaluate the impact of four STS modes, both with (WA) and without exoskeleton assistance (WOA), on the wearer's muscle strength.

Figure 4 reveals a consistent reduction in RMS of processed EMG signals across all subjects when comparing STS strategies under WA conditions to the WOA condition. This reduction is primarily seen in the left and right VL/BF muscles during low-speed STS exercises, indicating that virtual torque contributes significantly to reducing muscle activity and preventing failure in sit-back or step-like STS

DOI: 10.54254/2755-2721/41/20230702

movements. However, during moderate and sit-back-like STS exercises, no significant reduction in the EMG signal of the BF muscle is observed. In contrast, the EMG signal of the BF muscles significantly decreases during step-like STS exercises, attributed to the essential role of BF muscle contractions in maintaining balance during later stages of these exercises under WOA conditions. These findings suggest that the proposed impedance modulation control strategy holds promise for effectively reducing muscle activity in individuals with muscle weakness, thereby facilitating successful STS exercises.

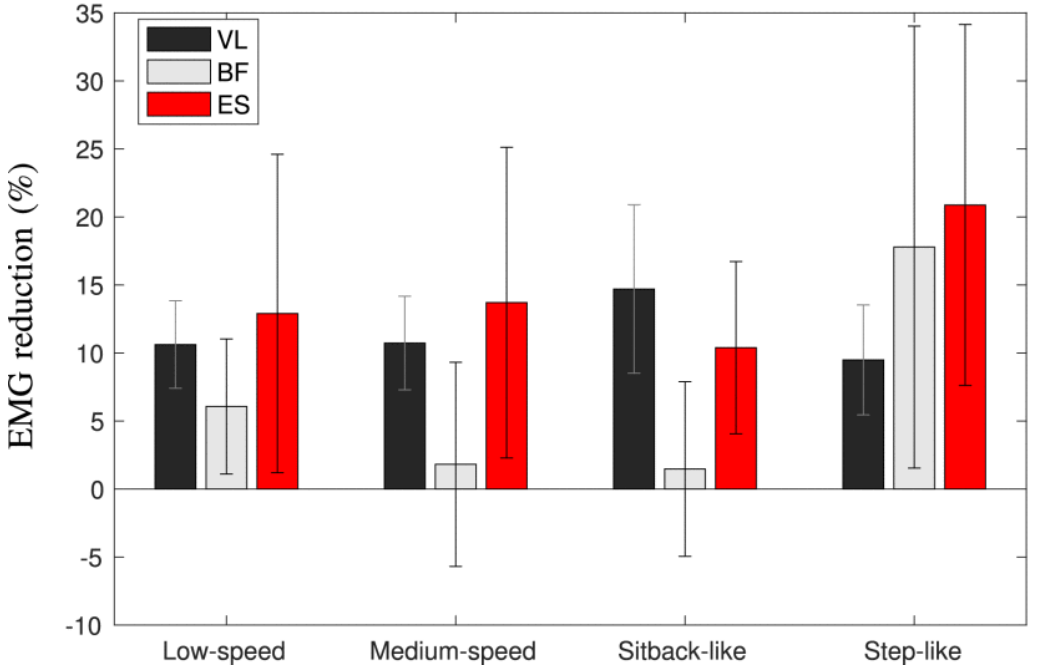

Figure 4. The average decrease in the RMS of processed EMG signals for all subjects across four types of STS strategies. 'VL' and 'BF' represent the average reduction in the left and right VL and BF muscles, respectively.

4. Conclusion

This article delves into two primary approaches for modeling mechanical exoskeleton control strategies aimed at assisting the elderly or those suffering from lower limb muscle weakness or paralysis in performing STS movements. The first approach mimics the natural trajectory of human legs during STS actions, ensuring the movement is neither forceful nor potentially harmful. It necessitates assistance for nearly all lower limb joints, employing a Kinematics architecture with a notable 18 DOF. Additionally, this approach employs a hybrid system model segregating STS motion into distinct sitting and standing phases to elevate user comfort. The second approach emphasizes decreasing the exertion on the user's legs. The support is mainly concentrated on the knee and hip joints, with the ankle joint remaining passive. From a modeling perspective, a triple inverted pendulum-based dynamic modeling is employed. This strategy also integrates a seat force model to discern when the user is poised for an STS action. To validate the real-world applicability and effectiveness of the second strategy, the article evaluates related experimental data. The findings affirm its efficacy in diminishing the muscular effort needed for STS movements while ensuring stability.

References

[1] Dehail P, Bestaven E, Muller F, Mallet A, Robert B, Bourdel-Marchasson I and Petit J 2007 Kinematic and electromyographic analysis of rising from a chair during a “sit-to-walk” task in elderly subjects: Role of strength, *Clin. Biomech.,* **vol. 22**, no. 10, pp. 1096–1103

DOI: 10.54254/2755-2721/41/20230702

[2] Riley PO, Krebs DE and Popat R. 1997 Biomechanical analysis of failed sit-to-stand, *IEEE Trans. Rehabil. Eng.,* **vol. 5**, no. 4, pp. 353–359
[3] Patil G, Rigoli L, Richardson MJ, Kumar M and Lorenz T 2018 Momentum-based trajectory planning for lower-limb exoskeletons supporting sit-to-stand transitions, *Int. J. Intell. Robot. Appl.,* **vol. 2**, no. 2, pp. 180–192
[4] Mefoued S, Mohammed S, Amirat Y and Fried G 2012 Sit-to-stand movement assistance using an actuated knee joint orthosis, In: *Proc. 4th IEEE RAS EMBS Int. Conf. Biomed. Robot. Biomechatronics (BioRob),* pp. 1753–1758
[5] Rajasekaran V, Vinagre M and Aranda J 2017 Event-based control for sit-to-stand transition using a wearable exoskeleton, In: *Proc. Int. Conf. Rehabil. Robot.,* pp. 400–405
[6] Tanghe K, Harutyunyan A, Aertbeliën E, De Groote F, De Schutter J, Vrancx P and Nowé A 2016 Predicting seat-off and detecting start-of-assistance events for assisting sit-to-stand with an exoskeleton, *IEEE Robot. Autom. Lett.,* **vol. 1**, no. 2, pp. 792–799
[7] Karavas N, Ajoudani A, Tsagarakis N, Saglia J, Bicchi A and Caldwell D 2013 Tele-impedance based stiffness and motion augmentation for a knee exoskeleton device, In: *Proc. IEEE Int. Conf. Robot. Autom.,* pp. 2194–2200
[8] Huo W, Moon H, Alouane MA, Bonnet V, Huang J, Amirat Y, Vaidyanathan R and Mohammed S 2022 Impedance Modulation Control of a Lower-Limb Exoskeleton to Assist Sit-to-Stand Movements, *IEEE Trans. Robotics,* **vol. 38**, no. 2, pp. 1230–1249. doi: 10.1109/TRO.2021.3104244
[9] Mungai ME and Grizzle JW 2021 Feedback Control Design for Robust Comfortable Sit-to-Stand Motions of 3D Lower-Limb Exoskeletons, *IEEE Access,* **vol. 9**, pp. 122–161. doi: 10.1109/ACCESS.2020.3046446
[10] *Atalante*. Apr. 2020 [Online]. Available: https://www.wandercraft.eu/en/exo/
[11] Spong MW, Hutchinson S and Vidyasagar M 2006 *Robot Modeling and Control*. (Hoboken, NJ, USA: Wiley)
[12] Sardain P and Bessonnet G 2004 Forces acting on a biped robot. Center of pressure—Zero moment point, *IEEE Trans. Syst. Man Cybern. A Syst. Humans,* **vol. 34**, no. 5, pp. 630–63
[13] Kajita S and Espiau B 2008 Legged robots. In: *Springer Handbook of Robotics,* Springer, pp. 361–389. [Online]. Available: https://doi.org/10.1007/978-3-540-30301-5_17
[14] Bonnet V and Venture G 2015 Fast determination of the planar body segment inertial parameters using affordable sensors, *IEEE Trans. Neural Syst. Rehabil. Eng.,* **vol. 23**, no. 4, pp. 628–635
[15] Grün M and Konigorski U 2012 *Observer based method for joint torque estimation in active orthoses. Math. Model.,* **vol. 7**, no. 1, pp. 199–204
[16] Craig JJ 2005 *Introduction to Robotics: Mechanics and Control.* (Upper Saddle River, NJ, USA: Prentice-Hall)